AD_____

Award Number: W81XWH-12-1-0629

TITLE: Novel Genetic Models to Study the Role of Inflammation in Brain Injury-Induced Alzheimer's Pathology

PRINCIPAL INVESTIGATOR: Bruce Lamb

CONTRACTING ORGANIZATION:

The Cleveland Clinic Foundation
Cleveland, OH 44195

REPORT DATE: October 2013

TYPE OF REPORT: Annual Report

PREPARED FOR: U.S. Army Medical Research and Materiel Command
Fort Detrick, Maryland 21702-5012

REPORT DOCUMENTATION PAGE

Form Approved
OMB No. 0704-0188

1. REPORT DATE	2. REPORT TYPE	3. DATES COVERED
01/Oct//2013	Annual	30 Sep 2012 – 29 Sep 2013

4. TITLE AND SUBTITLE

Novel Genetic Models to Study the Role of Inflammation in Brain Injury-Induced Alzheimer's Pathology

5a. CONTRACT NUMBER

5b. GRANT NUMBER
W81XWH-12-1-0629, EDMS 5629

5c. PROGRAM ELEMENT NUMBER

6. AUTHOR(S)
Bruce T. Lamb; Olga Kokiko-Cochran

E-Mail: lambb@ccf.org; kokikoo@ccf.org

5d. PROJECT NUMBER

5e. TASK NUMBER

5f. WORK UNIT NUMBER

7. PERFORMING ORGANIZATION NAME(S) AND ADDRESS(ES)

The Cleveland Clinic Foundation
9500 Euclid Avenue
Cleveland, OH 44195

8. PERFORMING ORGANIZATION REPORT NUMBER

9. SPONSORING / MONITORING AGENCY NAME(S) AND ADDRESS(ES)
U.S. Army Medical Research and Materiel Command
Fort Detrick, Maryland 21702-5012

10. SPONSOR/MONITOR'S ACRONYM(S)

11. SPONSOR/MONITOR'S REPORT NUMBER(S)

12. DISTRIBUTION / AVAILABILITY STATEMENT
Approved for Public Release; Distribution Unlimited

13. SUPPLEMENTARY NOTES

14. ABSTRACT
Individuals exposed to traumatic brain injury (TBI) are at a greatly increased risk for developing a number of neurodegenerative diseases including Alzheimer's disease (AD). TBI promotes the development of the pathological hallmarks of AD including production and extracellular deposition of the beta -amyloid peptide in senile plaques and intracellular aggregation of hyperphosphorylated, microtubule-associated protein tau (MAPT) in neurofibrillary tangles (NFTs). Several lines of evidence suggest that altered monocyte infiltration and microglial activation may be directly involved in the pathogenesis of both beta-amyloid and MAPT pathologies. The primary hypothesis to be tested in the current studies is that TBI induces infiltration of peripheral monocytes as well as acute and local activation of brain microglia within the injured brain and that these two cell types play roles distinct from each other in inducing both beta-amyloid pathologies and MAPT phosphorylation and aggregation leading to chronic pathological conditions that pre-dispose individuals exposed to TBI to develop AD later in life. Here we report that TBI results in brain cavitation and a widespread neuroinflammatory response including microglial activation and monocyte infiltration. Interestingly, the acute macrophage response to TBI is reduced in a mouse model of amyloid pathology (R1.40) compared to control mice; however, long-term behavioral outcome and neurodegeneration are worse at chronic postinjury time points. By contrast, pilot data examining TBI in hTau mice revealed increased phosphorylation of tau within neurons as well as enhanced microglial activation including swollen cell bodies and thickened processes when compared to brain injured controls. Recent data suggests that the macrophage response is also enhanced in brain injured hTau mice at acute postinjury time points. Taken together, these novel results suggest that TBI impacts amyloid and MAPT pathologies quite differently and have implications for immunomodulatory therapies for TBI.

15. SUBJECT TERMS
Alzheimer's, brain injury, beta-amyloid, MAPT, inflammation, monocytes, microglia

16. SECURITY CLASSIFICATION OF:			17. LIMITATION OF ABSTRACT	18. NUMBER OF PAGES	19a. NAME OF RESPONSIBLE PERSON
a. REPORT	b. ABSTRACT	c. THIS PAGE			USAMRMC
U	U	U	UU	14	19b. TELEPHONE NUMBER *(include area code)*

Table of Contents

Introduction

Exposure to traumatic brain injury (TBI) has numerous acute and chronic sequelae, including an increased risk for the development of Alzheimer's disease (AD)[1-3]. Mechanisms contributing to these pathological events are not well characterized; however, they are often associated with neuroinflammation. Postinjury neuroinflammation is characterized by activation of brain-resident microglia as well as infiltration and activation of monocytes due to disruption of the blood-brain barrier [4-6]. Assessing the exact roles of these cells in AD pathogenesis has proven exceedingly difficult as no immunohistochemical markers unambiguously differentiate monocytes from microglia, particularly in the activated (macrophage) state. Although there is increasing experimental evidence that macrophages derived from recruited monocytes can regulate Aβ pathologies, the effects of monocytes on other AD phenotypes, or the role of these cells in TBI induced AD pathologies have yet to be established. The central hypothesis of the current studies is that monocytes and microglia play roles decisively distinct from each other in the development of AD-like pathologies following TBI. Furthermore, these functions are exerted differentially in the varied pathological processes that underlie AD, including generation and extracellular deposition of beta-amyloid (Aβ) and phosphorylation and intracellular aggregation of microtubule associated protein tau (MAPT).

Body

Upon receipt of this award, we prepared and submitted a protocol to the Cleveland Clinic Institutional Animal Care and Use Committee (IACUC), which contained a detailed description of all studies proposed in the grant. The protocol was approved after minor revisions. The same animal use protocol was reviewed by the USMRMC Office of Research Protections. After additional minor revisions, including clarification of multiple survival surgeries and animal monitoring, all procedures were approved.

Specific Aim 1: Examine the spatial and temporal appearance of neuroinflammation and β-amyloid (Aβ) pathologies, cognitive deficits and neurodegeneration in R1.40 mice subjected to the lateral fluid percussion injury (FPI) paradigm of TBI

Statement of Work:

Task 1. Generate animals required for studies (timeframe, months 2-4)
Task 2. Perform FPI (timeframe, months 4-8)
Task 3. Perform behavioral analysis (timeframe, months 4-10)
Task 4. Analysis of brain tissue (timeframe, months 4-10)
Task 5. Published manuscript on results from Specific Aim 1 (timeframe, months 10-16)

The Lamb lab has generated the R1.40 mouse model of AD, which contains a full genomic copy of the human amyloid precursor protein (*APP*) gene with a familial AD mutation and develops age-related appearance of Aβ pathology at 12 months of age as well as earlier biochemical, neuropathological, and behavioral features of human AD [7, 8]. The R1.40 model is used extensively in the Lamb lab and therefore we were able to easily generate the animals required for the proposed studies. All R1.40 and non-transgenic animals (C57BL/6J, [B6]) generated were aged to two-months old before being surgically prepared for sham injury or lateral FPI resulting in four injury groups: R1.40 Sham, R1.40 TBI, B6 Sham, B6 TBI. Half of the animals in each group were aged to the acute 3 days postinjury (DPI) time point and the other half were aged to the chronic 120 DPI time point. Animals aged to 120 DPI completed motor and cognitive tests prior to sacrifice. At the selected time points, all mice were transcardially perfused and brain tissue was subsequently processed for neuropathological or biochemical analysis to document changes in postinjury neuroinflammation and AD-like Aβ pathology.

TBI Induces an Age-Dependent Increase in the Brain Injury Cavitation in R1.40 Mice

FPI induced extensive damage to the cortex that extended into the hippocampus at the site of injury, while sham animals did not display any obvious cortical damage (Fig. 1A). At 3 DPI, no significant differences in lesion volume were detected between Non-Tg and R1.40 TBI mice (Fig. 1B). At 120 DPI, an enlarged cavity was observed at the site of FPI in both genotypes (Fig. 1A). Notably, however, there was a statistically significant increase in lesion volume at 120 DPI when compared to the lesion volume observed at 3 DPI in TBI R1.40 mice only (Fig. 1B). Taken together, these data suggest that R1.40 mice exhibit a time-dependent enhancement in post-injury neurodegeneration, which could be due to alterations in neuroinflammatory reactions to TBI.

Brain injury induces region- and time-dependent changes in microglial activation

As expected, TBI induced alterations in microglial morphology in all brain regions examined at 3 DPI (Fig. 1C) when compared to sham controls. Form factor (FF) analysis of the brain sections, confirmed that microglial activation was significantly higher in TBI mice when compared to shams at 3DPI in the ipsilateral cortex and thalamus (Fig. 1D). By 120 DPI, FF analysis revealed reduced microglial activation in TBI mice within the ipsilateral cortex (Fig. 1E); however, microglial activation remained elevated in the ipsilateral thalamus in both Non-Tg and R1.40 animals exposed to TBI when compared to sham controls (Fig. 1F). Taken together, these findings demonstrate that cortical microglial activation dramatically decreases between 3DPI and 120DPI, although subcortical brain regions are at risk for sustained alterations in microglial activation. These results clearly demonstrate that TBI induces widespread microglial activation around the site of injury at 3 DPI and to a lesser extent at 120 DPI. No significant differences in FF analyses were observed between R1.40 and Non-Tg TBI mice at either time point, suggesting that the morphological state of microglia is similar between genotypes. However, since Iba1 immunohistochemistry recognizes both microglia as well as infiltrating monocytes, these studies could not discriminate between the effects of TBI on either microglia or monocytes.

Altered acute inflammatory response in R1.40 mice exposed to TBI

The leukocyte common antigen CD45, is differentially expressed within microglia and monocytes. CD45 expression is low in quiescent microglia and increases during microglial activation, whereas CD45 expression is high in blood-born monocytes [9, 10]. Not surprisingly, CD45 staining revealed the presence of brain microglia and/or infiltrating monocytes near the injury cavity at 3 DPI in TBI mice when compared to shams (Fig. 2A). However, there was a surprising reduction in CD45 immunoreactivity in brain injured R1.40 mice compared to brain injured Non-Tg mice in the ipsilateral thalamus (Fig. 2B). These findings suggest that the post-injury glial response was altered in the R1.40 mice and that microglia and/or monocytes differentially respond to TBI in the presence of accumulating APP and Aβ present in this model. The cell surface glycoprotein F4/80 is highly expressed on the surface of macrophages and is also widely used as a marker for microglia [11]. Similar to CD45, F4/80 staining was localized around the injury site in both Non-Tg and R1.40 mice when compared to sham controls at 3 DPI (Fig. 2C). Notably, there was a consistent reduction in F4/80 immunostaining in all brain regions examined in R1.40 TBI mice compared to Non-Tg TBI mice (Fig. 2D). Together, the CD45 and F4/80 staining, suggests that exposure of R1.40 mice to TBI results in an altered microglial/monocytic inflammatory response when compared to injured controls at early time points.

Finally, flow cytometry was used to quantify the accumulation of microglia and monocytes in the injured hemisphere at 3 DPI. Microglia and monocytes were isolated from separate groups of mice and stained for CD45 and F4/80 (Fig.2E-2F). A similar proportion of microglia positive for $CD45^{low}$ and F4/80 was identified in all groups (Fig. 2G). Although Non-Tg TBI mice showed a proportional increase in the number of monocytes positive for $CD45^{high}$ and F4/80 compared to all other groups, no significant differences were detected between any groups (Fig. 2H). Consistent with our immunohistochemical findings, the total percentage of F4/80 positive cells was significantly reduced in the TBI R1.40 mice compared to TBI Non-Tg mice (Fig. 2I). These data show that a similar proportion of microglia and monocytes are present in the brains of R1.40 TBI mice, but the macrophage response is reduced compared to Non-Tg TBI mice.

To examine the effects of TBI on chronic effects on microglia and monocytes, brain sections from both Non-Tg and R1.40 animals at 120 DPI were immunostained with CD45 and F4/80 (Fig. 2J, 2L). Not surprisingly, CD45 immunoreactivity was substantially reduced at 120 DPI compared to 3 DPI in TBI mice. No significant differences were detected between brain injured and sham animals at 120 DPI in the ipsi-cortex or conta-CA2 brain regions. However, within the ipsi-thalamus, CD45 immunostaining remained elevated in TBI animals at 120 DPI although no significant differences were detected between the Non-Tg and R1.40 animals exposed to TBI (Fig. 2K). Finally, F4/80 immunoreactivity was also reduced in Non-Tg brain injured mice at 120 DPI compared to 3 DPI (Fig. 2L). At 120 DPI there was no significant difference in F4/80 immunoreactivity between TBI Non-Tg and R1.40 mice; however, both brain injured groups showed heightened F4/80 immunoreactivity compared to sham animals in all regions analyzed (Fig. 2M). Interestingly, the expression profile of F4/80 was similar in all brain regions examined in R1.40 TBI mice at 3 DPI and 120 DPI. Together these data suggest that the presence of accumulating Aβ in R1.40 mice significantly alters the macrophage response to TBI at both acute and chronic time points.

Acute increase in postinjury APP expression declines at chronic time point.

To quantitate changes in postinjury APP levels, ipsilateral cortical extracts from separate groups of TBI and sham injured Non-Tg and R1.40 mice were probed with antibodies CT15 and 6E10 at 3DPI and 120DPI (Fig.

3A, 3D). Full-length APP expression significantly increased at 3 DPI in Non-Tg TBI mice compared to Non-Tg sham mice. APP expression was significantly higher in R1.40 mice compared to Non-Tg mice regardless of injury group (Fig. 3B); however, no significant differences in full-length APP expression were detected between R1.40 TBI and sham mice at 3 DPI (Fig. 3B-3C). By 120 DPI, full-length APP expression was significantly reduced in Non-Tg TBI mice compared to Non-Tg sham mice (Fig. 3E). APP expression continued to be higher in R1.40 mice compared to Non-Tg mice at 120 DPI (Fig. 3E), but a significant reduction in full-length human APP was also detected in R1.40 TBI mice compared to R1.40 sham mice (Fig. 3F). Given APP's postulated neurotrophic functions, a reduction in APP could compromise axonal sprouting, neuronal function, and synaptogenesis at later time points.

Brain injury induces time-dependent behavioral deficits.

To examine the chronic effects of TBI-induced neuroinflammation in promoting AD-like behavioral phenotypes, routine motor and cognitive tests were performed as mice aged to 120 DPI. The rotarod test was used to examine motor function. All mice performed similarly during baseline training, but TBI mice fell off of the rotating rod much faster than sham animals during the first week after injury. Notably, TBI mice continued to exhibit deficits in rotarod performance several months after TBI. Although we detected statistically significant differences between TBI and sham injured animals within each genotype, there were no differences in performance between B6 and R1.40 groups (Fig 4. A-B).

Spatial working memory was evaluated via an examination of spatial alternation in the Y maze. R1.40 animals exposed to TBI exhibited an age-dependent decline in working memory that reached statistical significance by 90 DPI, whereas B6 animals exposed to TBI did not exhibit an impairments at any age examined (Fig. 4C) or when compared to sham counterparts (data not shown). Importantly, there were no significant differences in arm entries between brain injured groups at any testing time point suggesting that motor deficits did not interfere with cognitive assessment (Fig. 4D).

Finally, spatial reference memory was assessed in the hidden platform version of the Morris water maze (MWM) beginning at 120 DPI. As expected, TBI resulted in longer latencies to reach the hidden goal platform in both Non-Tg and R1.40 mice; however, only Non-Tg TBI mice took significantly longer to reach the goal platform than Non-Tg sham injured animals across testing days (Fig. 4E). Surprisingly, no significant differences in latency to reach the platform were detected across testing days between R1.40 brain and sham injured mice (Fig. 4F) suggesting that both groups were able to learn the location of the platform. Finally, no group differences were observed in average swim speed or latency to reach a visible platform (data not shown), suggesting there were no motor or visual deficits that could act as confounding variables.

The water maze is an integrative task that requires a number of cognitive processes working in conjunction, including encoding, consolidation, storage, and retrieval, all of which are distinct memory processes. To better assess these behavioral components we utilized two different learning indices to quantify within- and between-day learning. The acquisition index, which measures within-day learning, in Non-Tg TBI mice was less than one suggesting that the time to reach the goal platform was similar between trial 1 and trial 4 within any given memory testing day. Surprisingly, the acquisition index in R1.40 TBI mice averaged around 13, and was significantly higher than brain injured Non-Tg mice (Fig. 4G). This finding demonstrates that R1.40 TBI mice show tremendous improvement in performance between trial 1 and trial 4 within any given memory testing day.

Next, we utilized a savings index, which quantifies how much learned information is transferred or "saved" across days, and provides an indirect measure of memory consolidation. The savings index in Non-Tg TBI mice averaged around two, indicating that there was only slight improvement from one day to the next in the latency to reach the goal platform. Interestingly, the savings index in R1.40 TBI mice averaged around negative six suggesting that performance significantly worsened from one day to the next (Fig. 4H). Together, these data demonstrate that Non-Tg and R1.40 TBI mice maintain unique profiles of within and between day learning in the water maze task even though average latency to reach the platform was similar. R1.40 mice display a deficit in transferring information from one day to the next but are able to overcome this deficit by quickly improving their performance within each day.

In conclusion, this study demonstrates that TBI induces a distinct neuroinflammatory response in the genomic-based R1.40 mouse model of AD. These experiments suggest that microglia in the presence of accumulating Aβ in the R1.40 mice respond differently to a secondary immune challenge such as TBI and the macrophage response is compromised. However, at more chronic time points following TBI, R1.40 mice exhibit enhanced neurodegeneration and also unique impairments in both working memory and components of memory consolidation and retrieval in spatial reference memory. These studies suggest that animals prone to develop AD exhibit a unique inflammatory response to TBI that has different short- and long-term

consequences. A further definition of the inflammatory response, including the role of infiltrating monocytes and microglia and different states of activation of these cells are required to gain insight into the potential factors that drive long-term functional outcome measures following TBI.

Specific Aim 2: Examine the spatial and temporal appearance of neuroinflammation and MAPT pathologies, cognitive deficits and neurodegeneration in hTau mice subjected to lateral FPI.

Statement of Work:
Task 1. Generate animals required for studies (timeframe, months 4-8)
Task 2. Perform FPI (timeframe, months 8-12)
Task 3. Perform behavioral analysis (timeframe, months 8-14)
Task 4. Analysis of brain tissue (timeframe, months 8-14)
Task 5. Published manuscript on results from Specific Aim 2 (timeframe, months 14-18)

Davies and colleagues developed a genomic mouse model of human MAPT pathology (termed hTau) by expressing the entire wild-type human *MAPT* gene in mice lacking the endogenous *Mapt* gene [12, 13]. hTau mice exhibit age-related accumulation of hyperphosphorylated human MAPT as well as altered neuronal cell cycle and cell death with appropriate localization, timing and neurotoxic effects. This unique model allows us to accurately study the effects of TBI induced inflammation on disease-relevant human MAPT pathology. The hTau model is used extensively in the Lamb lab; however, there have been some unforeseen difficulties in breeding over the past six months. As a result our initial efforts have been focused on utilizing the hTau and matched control mice to assess neuropathological changes at the acute 3 DPI time point. All hTau and B6 mice generated have been aged to two-months old before being surgically prepared for sham injury or lateral FPI resulting in four injury groups: hTau Sham, hTau TBI, B6 Sham, B6 TBI. At 3 DPI, all mice have been transcardially perfused and brain tissue was subsequently processed for neuropathological analysis. We are currently preparing the final samples for quantitative analysis. Importantly, the hTau breeding has improved and we have begun aging animals to the chronic 120 DPI time point. Behavioral testing has begun, although no data has been analyzed at this time.

Specific Aim 3: Identify, track, purify and analyze gene expression profiles on infiltrating monocytes and resident microglia at different stages of Aβ and MAPT pathologies following TBI.

Statement of Work:
Task 1. Generate animals required for studies (timeframe 8-12 months)
Task 2. Perform FPI (timeframe, months 12-20)
Task 3. Analysis of brain tissue (timeframe, months 12-20)
Task 4. Purification of monocytes/microglia (timeframe, months 12-20)
Task 5. Gene expression microarray analysis (timeframe, months 12-24)
Task 6. Multi-photon microscopy (timeframe, months 12-24)
Task 7. Published manuscript on results from Specific Aim 1 (timeframe, months 20-24)

In blood, two non-overlapping monocyte populations are distinguished by differential expression of two chemokine receptors and surface glycoprotein Ly6C (Ly6C^{hi}/CX3CR1^{low}/CCR2+ and Ly6C^{low}/CX3CR1^{hi}/CCR2-negative)[14, 15]. No tissue-immunohistochemistry markers unambiguously differentiate monocytes from microglia, particularly in the activated (macrophage) state [16]. However, our laboratories have recently performed pioneering studies using genetic labels regulated by these chemokine-receptor promoters to show that, serendipitously, CX3CR1 and CCR2 distinguish microglia from monocytes in the inflamed CNS [17]. This distinction arose from the following observations:

- Monocyte expression of CCR2, responding the chemokine ligand CCL2, is functionally required for monocytes to enter the CNS and therefore CNS-infiltrating monocytes are CCR2+;
- CX3CR1 is expressed by microglia from their first entry into the neuroepithelial parenchyma around E10 until adulthood, when microglia remain uniformly CX3CR1+. Furthermore, microglia do not express CCR2 or downregulate CX3CR1, even during severe neuroinflammation.

Cx3cr1$^{GFP/+}$/Ccr2$^{RFP/+}$ mice provided a first opportunity to evaluate differential microglial and monocyte contributions to acute neuroinflammation by correlating gene expression of sorted monocytes and microglia with protein localization by immunohistochemistry (IHC). Cx3cr1$^{GFP/+}$/Ccr2$^{RFP/+}$ mice were readily available within the Lamb and Ransohoff labs; however, R1.40/ Cx3cr1$^{GFP/+}$/Ccr2$^{RFP/+}$ and hTau/ Cx3cr1$^{GFP/+}$/Ccr2$^{RFP/+}$

were not. Thus, we have focused our efforts on breeding these genotypes over the past six months. We currently have a stock supply of age matched Cx3cr1$^{GFP/+}$/Ccr2$^{RFP/+}$ and R1.40/ Cx3cr1$^{GFP/+}$/Ccr2$^{RFP/+}$ mice in our colony and have begun administered TBI and sham injury to two-month old animals. Several brain tissue samples have been collected at the acute 3 DPI time point and several other animals are aging to the chronic 120 DPI time point. We began breeding the hTau/ Cx3cr1$^{GFP/+}$/Ccr2$^{RFP/+}$ mice approximately three months ago and will have the first animals for surgery next month. We have been optimizing our flow cytometry protocol while animals are breeding to insure efficient and accurate processing of samples when they are available.

Key Research Accomplishments

- Received approval from Cleveland Clinic IACUC for all studies included in proposal, Approval 28-09-2012.
- Received approval from the US Army Medical Research and Material Command (USAMRMC) Animal Care and Review Office (ACURO) Protections for all studies included in the proposal, Approval 18-10-2012.
- Completed Milestone Specific Aim1
    a. Task 1: Generated R1.40 and B6 animals required for studies
    b. Task 2: FPI or sham injury was administered to two-month old R1.40 and B6 mice
    c. Task 3: Behavioral analysis was completed in two-month old R1.40 and B6 mice aged to 120 days postinjury (DPI)
    d. Task 4: Brain tissue from acute 3 DPI as well as chronic 120 DPI time points were collected and processed for neuropathology and biochemistry
    e. Task 5: Manuscript of studies included in Specific Aim 1 has been drafted and will be submitted for publication within the next month
- Initiated Milestone Specific Aim 2
    a. Task 1: Generated hTau and B6 mice required for studies
    b. Task 2: FPI or sham injury has been administered to several groups of two-month old hTau and B6 mice for acute 3 DPI time point
    c. Task 3: Behavioral analysis has begun with initial cohort of two-month old hTau mice aging to 120 DPI
    d. Task 4: Brain tissue from acute 3 DPI time point has been collected from hTau and B6 mice and is being processed for neuropathology
- Initiated Milestone Specific Aim 3
    a. Task 1: Generated CX3CR1$^{GFP/+}$/CCR2$^{RFP/+}$, R1.40/ CX3CR1$^{GFP/+}$/CCR2$^{RFP/+}$, and hTau/ CX3CR1$^{GFP/+}$/CCR2$^{RFP/+}$ mice
    b. Task 2: FPI or sham injury has been administered to initial CX3CR1$^{GFP/+}$/CCR2$^{RFP/+}$ and R1.40/ CX3CR1$^{GFP/+}$/CCR2$^{RFP/+}$ mice, which are currently aging to 3 DPI or 120 DPI
    c. Task 3: Some brain tissue from acute 3DPI time point has been collected

Reportable Outcomes

Abstracts

- Kokiko-Cochran, O., Veenstra, M., Ransohoff, L., Bhaskar, K., Lee, Y-S, Lamb, B. “Traumatic brain injury distinctly influences amyloid and tau pathology”, Society for Neuroscience Conference, New Orleans, LA, October, 2012.
- Kokiko-Cochran, O., Ransohoff, L., Bhaskar, K., Lee, Y-S, Lamb, B. “Traumatic brain injury induces a distinct inflammatory response in a genomic based model of Alzheimer’s disease”, National Neurotrauma Symposium, Nashville, TN, August, 2013.

Publications

- Manuscript describing experiments completed in Specific Aim 1 prepared “Opposing acute and chronic effects of traumatic brain injury in a mouse model of Alzheimer’s disease” to be submitted in the next few weeks.

Animal Models

- CX3CR1$^{GFP/+}$/CCR2$^{RFP/+}$, R1.40/ CX3CR1$^{GFP/+}$/CCR2$^{RFP/+}$, and hTau/ CX3CR1$^{GFP/+}$/CCR2$^{RFP/+}$ mice generated and available to requesting investigators. All models are also deposited at The Jackson Laboratory.

Grant Funding

- NINDS R21, NS087298, PIs: B.T. Lamb and R.M. Ransohoff, “The Role of Monocytes and Microglia in Traumatic Brain Injury-Induced Tauopathies, 7/1/13-6/30/15.
- TATRC MRPRA, ERMS#13321017, PIs: L. Goldstein and B.T. Lamb, “Effects of Blast Neurotrauma on Alzheimer’s Disease Pathogenesis, 10/1/13-9/31/15.

Conclusion

Numerous studies have documented that prior incidence of TBI may gradually lead to AD-related pathologies, neuroinflammation, neurodegeneration and dementia. Since neuroinflammation is a rapid response to brain trauma, it is extremely important to understand specific contributions of microglia (resident immune cells of the brain) *versus* monocytes (bone-marrow derived immune cells) in mediating amyloid and MAPT pathology as well as cognitive impairment, which is often encountered in injured combatants. The first two specific aims include experiments to characterize the neuroinflammatory response in separate amyloid and tau mouse models of AD. Our data continues to suggest that the brain injury induced neuroinflammatory response impacts Aβ and MAPT pathologies quite differently, with only modest effects focused on altered microglial activation in a genomic-based model of Aβ pathologies, but dramatically enhanced MAPT phosphorylation and aggregation in a genomic-based model of MAPT pathologies, although proper quantification still needs to be completed. The final studies in this project will utilize and characterize unique genetic and genomic models to individually label microglia and monocytes so as to understand their relative contribution and functional roles in neurodegenerative processes. The outcome of this study will have a major impact in understanding the role of monocytes and microglia in AD-related pathologies following TBI. We will identify when these cells first appear following TBI, the genes expressed in each cell type and the spatial and temporal relationship to Aβ and MAPT pathologies. We currently have all genotypes necessary to finish this project and are well positioned to provide all deliverables listed in our Statement of Work included in the initial proposal.

References

1. Fujimoto, S.T., et al., *Motor and cognitive function evaluation following experimental traumatic brain injury.* Neurosci Biobehav Rev, 2004. **28**(4): p. 365-78.
2. Tokuda, T., et al., *Re-examination of ex-boxers' brains using immunohistochemistry with antibodies to amyloid beta-protein and tau protein.* Acta Neuropathol, 1991. **82**(4): p. 280-5.
3. Guo, Z., et al., *Head injury and the risk of AD in the MIRAGE study.* Neurology, 2000. **54**(6): p. 1316-23.
4. Pierce, J.E., et al., *Enduring cognitive, neurobehavioral and histopathological changes persist for up to one year following severe experimental brain injury in rats.* Neuroscience, 1998. **87**(2): p. 359-69.
5. Smith, D.H., et al., *Progressive atrophy and neuron death for one year following brain trauma in the rat.* J Neurotrauma, 1997. **14**(10): p. 715-27.
6. Soares, H.D., et al., *Inflammatory leukocytic recruitment and diffuse neuronal degeneration are separate pathological processes resulting from traumatic brain injury.* J Neurosci, 1995. **15**(12): p. 8223-33.
7. Lamb, B.T., et al., *Altered metabolism of familial Alzheimer's disease-linked amyloid precursor protein variants in yeast artificial chromosome transgenic mice.* Hum Mol Genet, 1997. **6**(9): p. 1535-41.
8. Lamb, B.T., et al., *Introduction and expression of the 400 kilobase amyloid precursor protein gene in transgenic mice [corrected].* Nat Genet, 1993. **5**(1): p. 22-30.
9. Carson, M.J., et al., *Mature microglia resemble immature antigen-presenting cells.* Glia, 1998. **22**(1): p. 72-85.
10. Campanella, M., et al., *Flow cytometric analysis of inflammatory cells in ischemic rat brain.* Stroke, 2002. **33**(2): p. 586-92.
11. Lin, H.H., et al., *F4/80: the macrophage-specific adhesion-GPCR and its role in immunoregulation.* Adv Exp Med Biol, 2010. **706**: p. 149-56.
12. Andorfer, C., et al., *Cell-cycle reentry and cell death in transgenic mice expressing nonmutant human tau isoforms.* J Neurosci, 2005. **25**(22): p. 5446-54.
13. Andorfer, C., et al., *Hyperphosphorylation and aggregation of tau in mice expressing normal human tau isoforms.* J Neurochem, 2003. **86**(3): p. 582-90.
14. Geissmann, F., et al., *Unravelling mononuclear phagocyte heterogeneity.* Nat Rev Immunol, 2010. **10**(6): p. 453-60.

15. Geissmann, F., S. Jung, and D.R. Littman, *Blood monocytes consist of two principal subsets with distinct migratory properties.* Immunity, 2003. **19**(1): p. 71-82.
16. Ransohoff, R.M. and V.H. Perry, *Microglial physiology: unique stimuli, specialized responses.* Annu Rev Immunol, 2009. **27**: p. 119-45.
17. Saederup, N., et al., *Selective chemokine receptor usage by central nervous system myeloid cells in CCR2-red fluorescent protein knock-in mice.* PLoS One, 2010. **5**(10): p. e13693.

Appendices
N/A

Supporting Data

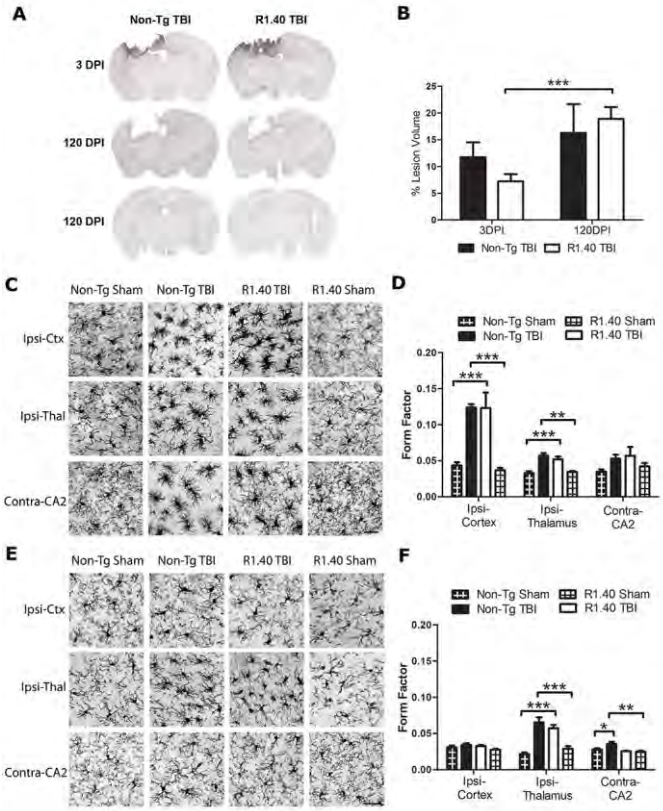

Figure 1. Time-dependent changes in lesion size and microglial activation. (A) Representative photomicrographs show a cortical injury cavity at 3 DPI in TBI mice, which is larger at 120 DPI. No visible lesion cavity is observed in sham mice (bottom row) at 120DPI. (B) Lesion analysis reveals a time-dependent increase in the size of the injury cavity in the R1.40 mice at 120DPI compared to 3 DPI. (C, E) Representative images of Iba1 immunostaining in sham and TBI mice in ipsilateral cortex (Ipsi-Ctx), ipsilateral thalamus (Ipsi-Thal), and contralateral CA2 (Contra-CA2) brain regions at 3 DPI and 120 DPI. (D) FF analysis of Iba1 positive microglia at 3 DPI revealed higher values in Non-Tg and R1.40 TBI mice compared to sham mice in the Ipsi-Ctx and Ipsi-Thal. (F) FF analysis at 120 DPI revealed higher values in the Ipsi-Thal of TBI animals compared to shams. Non-Tg TBI mice display higher FF values in the Contra-CA2 region compared to all other groups. Error bars indicate SEM. Scale bars indicate 20 μm. *, $p < 0.05$, **; $p < 0.01$; ***, $p < 0.001$.

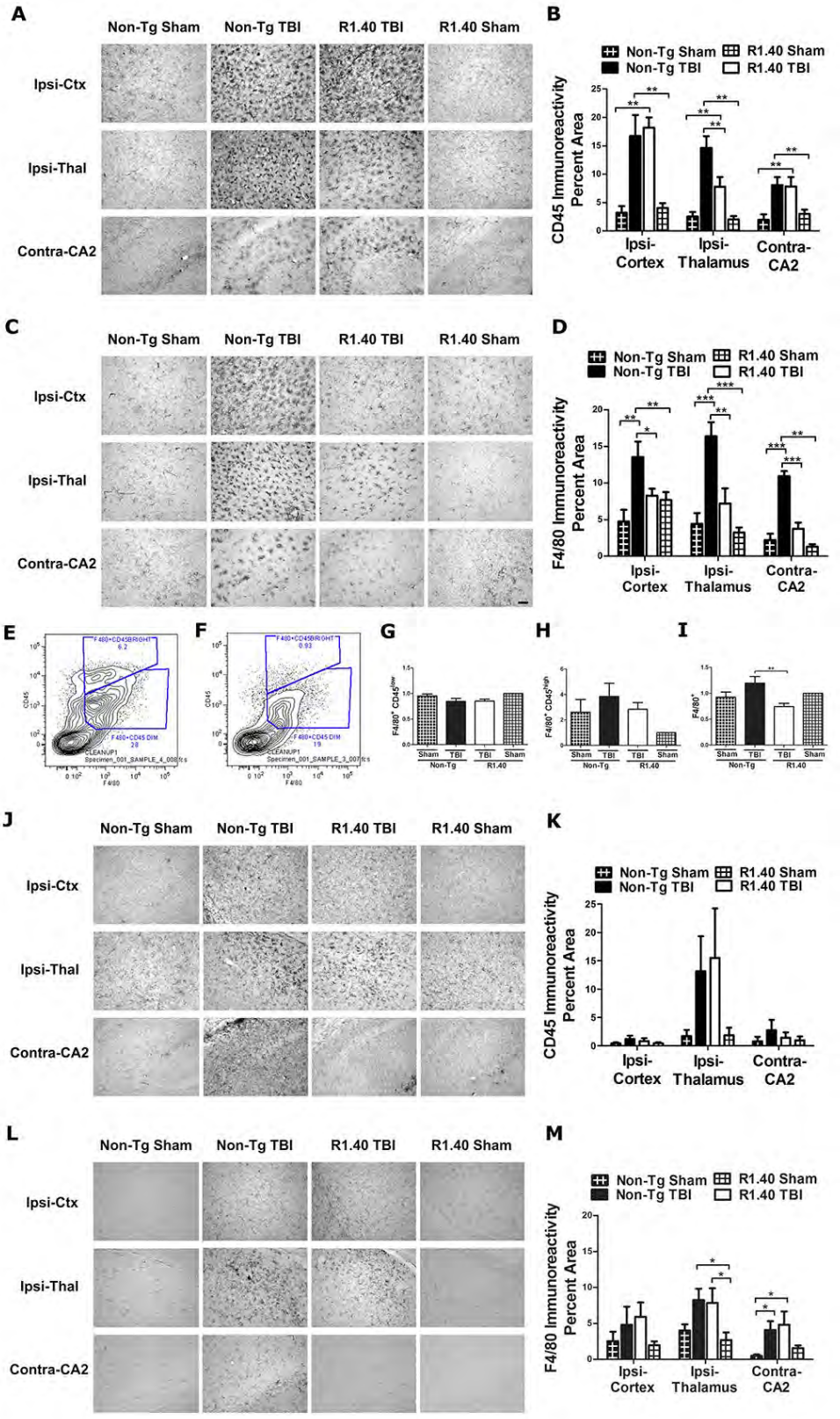

Figure 2. Distinct inflammatory response in brain injured R1.40 mice at 3DPI and 120DPI. (A, C) Representative images of CD45 and F4/80 immunostaining in sham and TBI mice in Ipsi-Ctx, Ipsi-Thal, and Contra-CA2 brain regions at 3 DPI. (B) Non-Tg and R1.40 TBI mice show similar levels of increased CD45 immunoreactivity compared to sham animals in all brain regions. R1.40 TBI mice showed a decrease in CD45 immunoreactivity compared to Non-Tg TBI mice in the Ipsi-Thal. (D) F4/80 immunoreactivity was significantly elevated in Non-Tg TBI mice compared to all other groups in each brain region analyzed. R1.40 TBI mice showed increased F4/80 immunoreactivity compared to R1.40 sham animals in the Contra-CA2 only. (E, F) Representative contour plots of microglia ($CD45^{low}$/F4/80 cells) and monocytes ($CD45^{high}$/F4/80 cells) in Non-Tg and R1.40 TBI mice at 3DPI. (G, H) Microglia and monocyte accumulation, respectively, in all groups at 3DPI. No significant differences were detected between TBI and sham mice. (I) R1.40 TBI mice show a significant decrease in $CD45^{+}$/$F4/80^{+}$ compared to Non-Tg TBI mice at 3DPI. (J, L) Representative images of CD45 and F4/80 immunostaining in sham and TBI mice at 120 DPI. (K) No significant differences in CD45 immunoreactivity were observed in any brain region analyzed, but CD45 immunoreactivity remained elevated in the Ipsi-Thal in both Non-Tg and R1.40 TBI mice. (D) No significant differences in F4/80 immunoreactivity were observed between groups in the Ipsi-Ctx, but F4/80 remained elevated in brain injured mice compared to sham mice in the Ipsi-Thal and Contra-CA2 regions at 120DPI. Error bars indicate SEM. Scale bars indicate 20 μm. *, $p < 0.05$, **; $p < 0.01$; ***, $p < 0.001$.

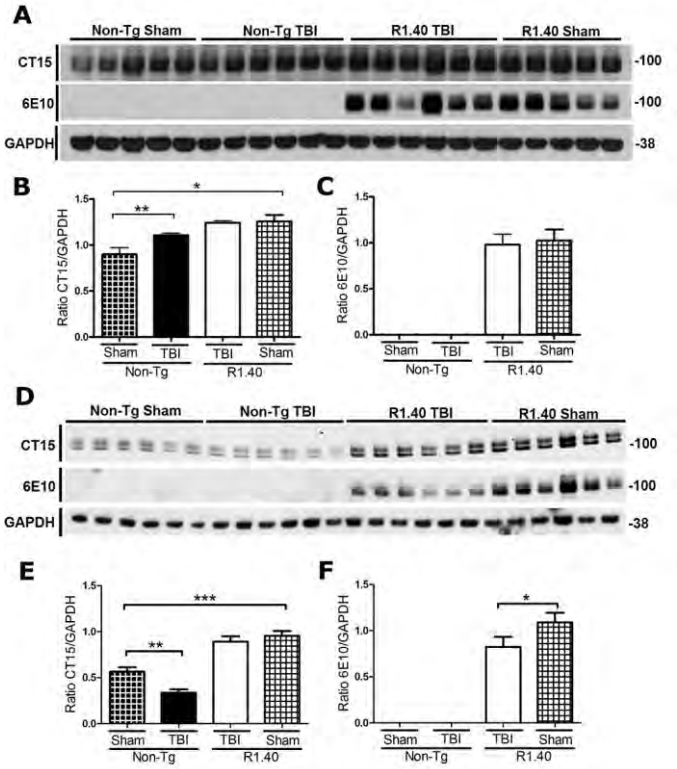

Figure 3. TBI causes time dependent changes in APP expression. (A, D) Western blot of cortical extracts were probed with antibodies CT15, 6E10, and GAPDH. (B) There was a significant increase in APP in Non-Tg TBI mice compared to Non-Tg shams at 3 DPI. R1.40 TBI mice displayed higher levels of APP than Non-Tg TBI mice, but no differences in APP expression were identified between R1.40 TBI and R1.40 sham mice at 3 DPI. (C) No difference in human APP expression was found between R1.40 TBI and R1.40 sham mice at 3 DPI. (E) There was a significant reduction in APP in Non-Tg TBI mice compared to Non-Tg shams at 120 DPI. APP levels were reduced in Non-Tg mice compared to R1.40 mice regardless of injury group. (F) R1.40 TBI mice displayed a significant reduction in human APP expression compared to R1.40 sham mice at 120 DPI. Error bars indicate SEM. *, $p < 0.05$; ***, $p < 0.001$.

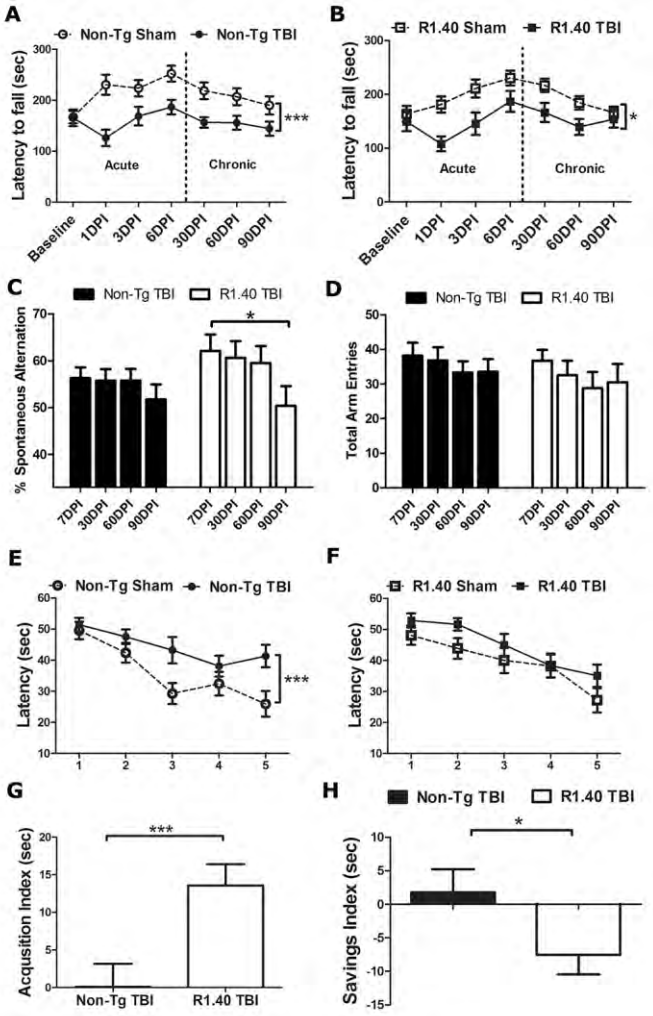

Figure 4. TBI induces time dependent changes in motor and cognitive function. (A, B) Mean latency to fall from the rotating rod was shorter in TBI mice at all postinjury time points compared to shams regardless of genotype. No between genotype differences in rotarod performance were detected in sham and TBI mice. (C) No significant differences between groups in average spontaneous alternation in the y maze. R1.40 TBI mice showed a significant reduction in percent spontaneous alternation between arms from 7 DPI to 90 DPI. (D) Average total arm entries were similar between TBI groups. (E) Non-Tg TBI mice displayed significantly longer mean latencies than Non-Tg sham mice to locate the hidden platform in the MWM at 120DPI. (F) No differences in mean latency to reach the hidden platform were detected between R1.40 TBI and sham mice at 120DPI. (G) Average acquisition index shows that latency to reach the platform significantly decreases within a testing day in R1.40 compared to Non-Tg mice. (D) Average savings index shows that latency to reach the platform significantly increases between testing days in R1.40 compared to Non-Tg mice. Error bars indicate SEM. *, $p < 0.05$; ***, $p < 0.001$.